An Updated Reaction Model for the High-Temperature Pyrolysis and Oxidation of Acetaldehyde

R. Mével[a,b,*], K. Chatelain[c,*], G. Blanquart[d], J.E. Shepherd[e]

[a] *Center for Combustion Energy, Tsinghua University, Beijing 100084, China*
[b] *Department of Automotive Engineering, Tsinghua University, Beijing 100084, China*
[c] *ENSTA-ParisTech, Paris-Saclay University, Palaiseau, France*
[d] *Mechanical Engineering Department, California Institute of Technology, Pasadena, CA, USA*
[e] *Graduate Aerospace Laboratories, California Institute of Technology, Pasadena, CA, USA*

This supplemental material presents the comparison between the complete set of experimental data and the predictions of the four detailed reaction models: (i) the present updated model, (ii) Aramco 2.0 [1], (iii) CaltechMech [2], and (iv) JetSurf [3]. The compositions and conditions are summarized in Table 1 of the manuscript. In Figure 1 to Figure 11, the predictions of the present model are shown as solid lines, the predictions of the Aramco 2.0 are shown as dashed-dotted lines, the predictions of CaltechMech are shown as dotted lines, and the predictions of JetSurf are shown as dashed lines.

*Corresponding author: mevel@mail.tsinghua.edu.cn

Delay-times

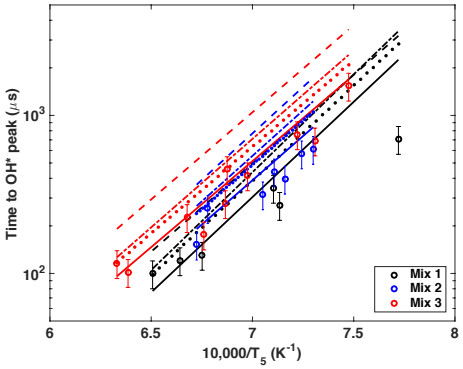

a) Delay-time based on OH* emission

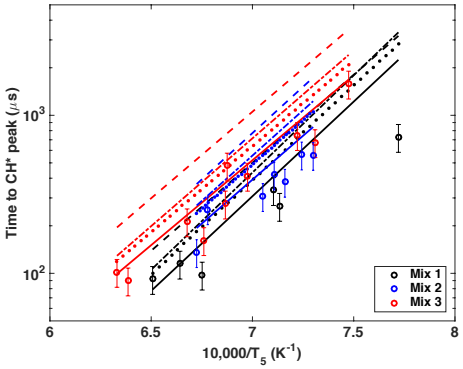

b) Delay-time based on CH* emission

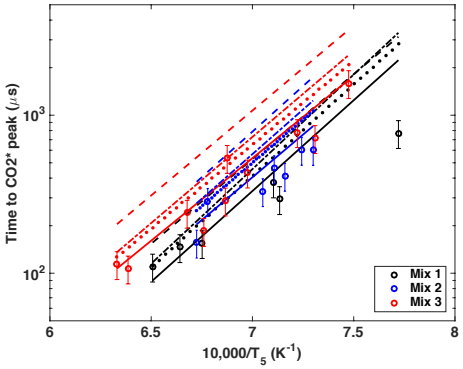

c) Delay-time based on CO_2* emission

Figure 1: Comparison between the experimental (present study) and calculated delay-time based on OH*, CH* and CO_2* for CH_3CHO-O_2-Ar mixtures. Solid lines: present model; Dashed-dotted lines: Aramco 2.0; Dotted lines: CaltechMech; Dashed lines: JetSurf.

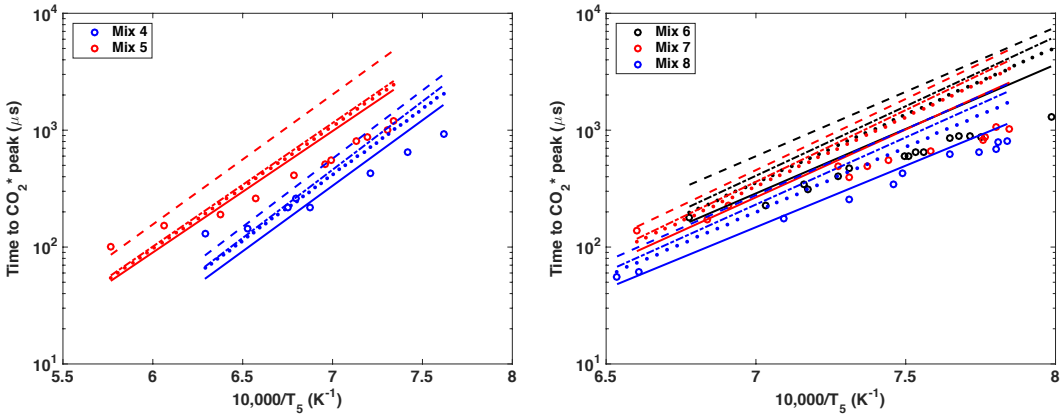

a) CO_2* emission at low pressure b) CO_2* emission at high pressure

Figure 2: Comparison between the experimental [4] and calculated delay-time based on CO_2* for CH_3CHO-O_2-Ar mixtures. Solid lines: present model; Dashed-dotted lines: Aramco 2.0; Dotted lines: CaltechMech; Dashed lines: JetSurf.

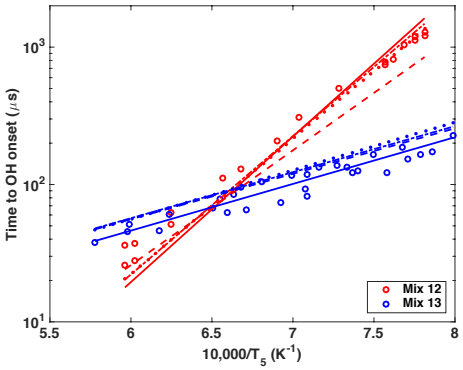

a) Delay-time based on OH absorption

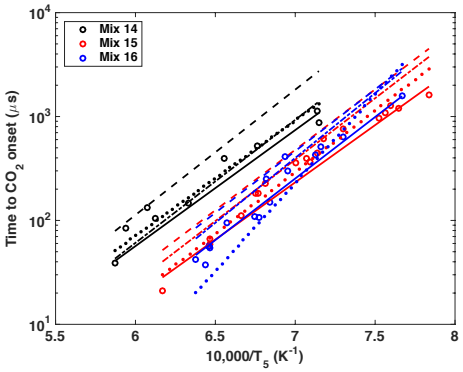

b) Delay-time based on CO_2 emission at 4.24 μm

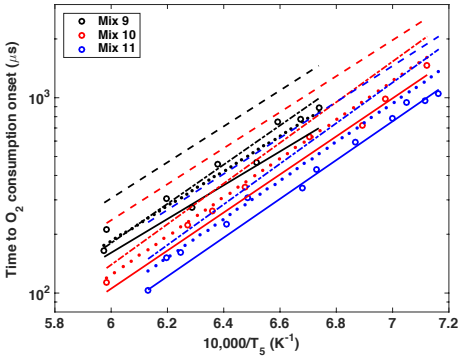

c) Delay-time based on O_2 (MS analysis)

Figure 3: Comparison between the experimental [5, 6] and calculated delay-time based on OH, CO_2 and O_2 for CH_3CHO-O_2-Ar mixtures with and without H_2 and a H_2-O_2-Ar mixture. Solid lines: present model; Dashed-dotted lines: Aramco 2.0; Dotted lines: CaltechMech; Dashed lines: JetSurf.

Species profiles

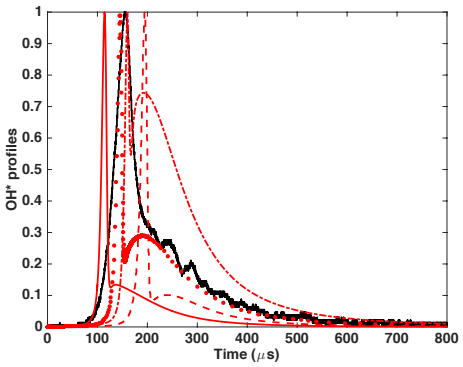

a) OH* profiles for mixture 1 at T_5=1506 K and P_5=339 kPa

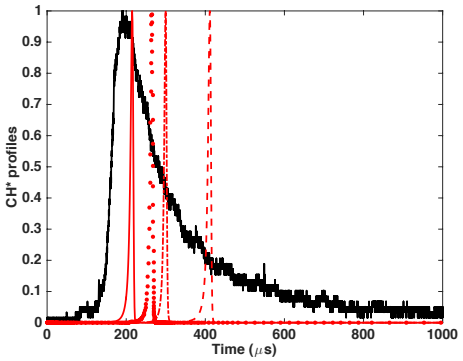

b) CH* profiles for mixture 2 at T_5=1475 K and P_5=356 kPa

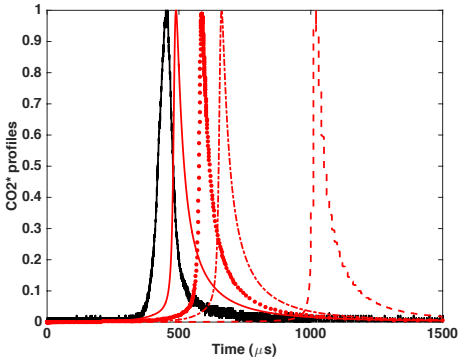

c) CO_2* profiles for mixture 3 at T_5=1434 K and P_5=342 kPa

Figure 4: Comparison between the experimental (present study) and the predicted OH*, CH* and CO_2* emission profiles during the oxidation of CH_3CHO. Solid lines: present model; Dashed-dotted lines: Aramco 2.0; Dotted lines: CaltechMech; Dashed lines: JetSurf.

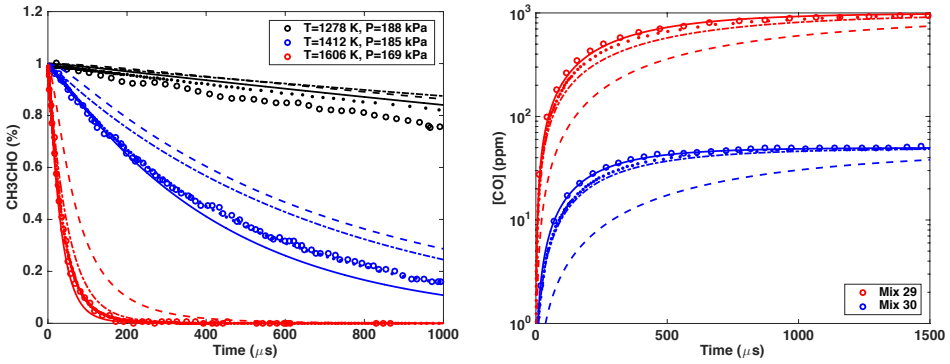

a) Laser absorption at 306.7 nm b) Laser absorption at 4.6 μm

Figure 5: Comparison between the experimental and the predicted CH_3CHO [7] and CO [8] profiles during the pyrolysis of CH_3CHO-Ar mixtures. Solid lines: present model; Dashed-dotted lines: Aramco 2.0; Dotted lines: CaltechMech; Dashed lines: JetSurf.

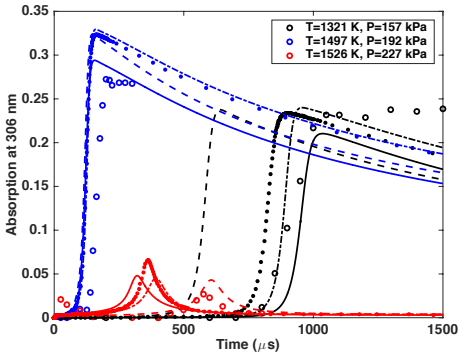

a) OH absorption (306.7 nm)

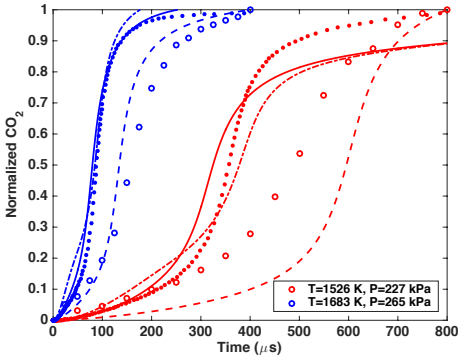

b) CO_2 emission (4.24 μm)

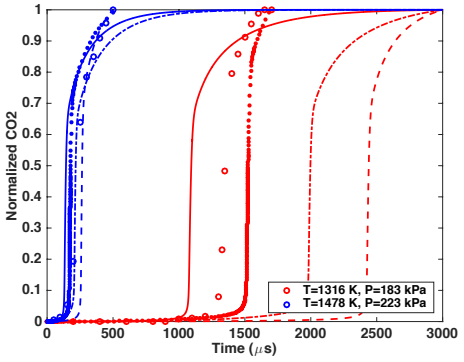

c) CO_2 emission (4.24 μm)

Figure 6: Comparison between the experimental [6] and the predicted OH absorption and CO_2 emission profiles for CH_3CHO-O_2-Ar mixtures with and without hydrogen and a H_2-O_2-Ar mixture. Mixture 12: ◯ and ◯, and Mixture 14: ◯ in a); Mixture 14: ◯ and ◯ in b); Mixture 15: ◯ and ◯ in c). Solid lines: present model; Dashed-dotted lines: Aramco 2.0; Dotted lines: CaltechMech; Dashed lines: JetSurf.

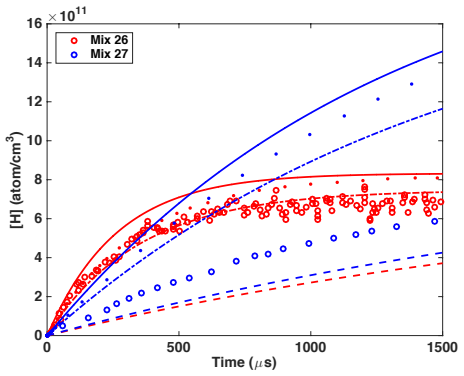

a) CH_3CHO pyrolysis [9]

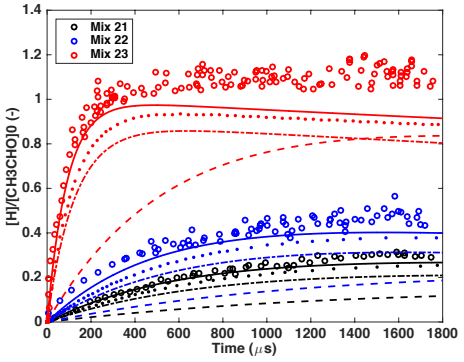

b) CH_3CHO pyrolysis [10]

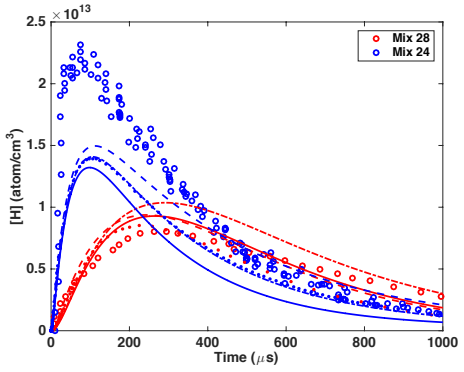

c) CH_3CHO-C_2H_5I pyrolysis [9, 10]

Figure 7: Comparison between the experimental and the predicted H atom profiles [9, 10] during the pyrolysis of CH_3CHO-Ar mixtures with and without C_2H_5I addition. In c), the experimental and calculated concentrations of H for mixture 28 has been multiplied by 10. Solid lines: present model; Dashed-dotted lines: Aramco 2.0; Dotted lines: CaltechMech; Dashed lines: JetSurf.

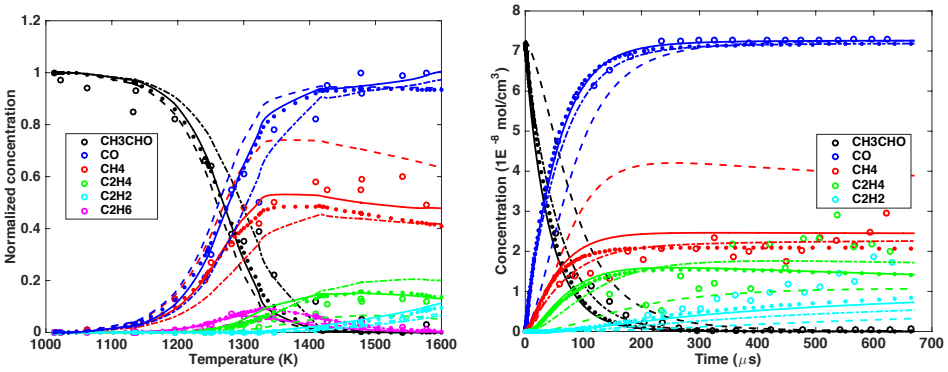

a) Sampling-GC analysis b) Time-resolved MS

Figure 8: Comparison between the experimental [6] and [11] and the predicted species profiles during the pyrolysis of CH_3CHO-Ar mixtures. Conditions: Mixture 18 in a) and Mixture 25 in b). Solid lines: present model; Dashed-dotted lines: Aramco 2.0; Dotted lines: CaltechMech; Dashed lines: JetSurf.

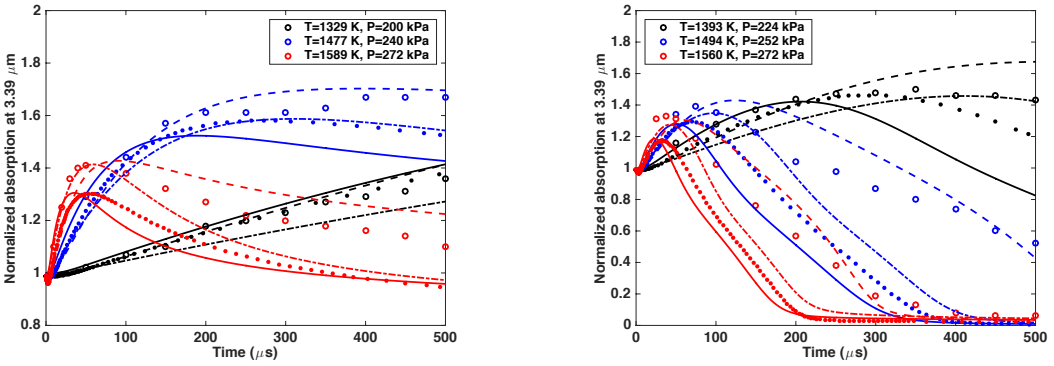

a) Absorption at 3.39 μm for mixture 19 b) Absorption at 3.39 μm for mixture 17

Figure 9: Comparison between the experimental [6] and the predicted absorption at 3.39 μm profiles during the pyrolysis (a) and oxidation (b) of CH_3CHO. Solid lines: present model; Dashed-dotted lines: Aramco 2.0; Dotted lines: CaltechMech; Dashed lines: JetSurf.

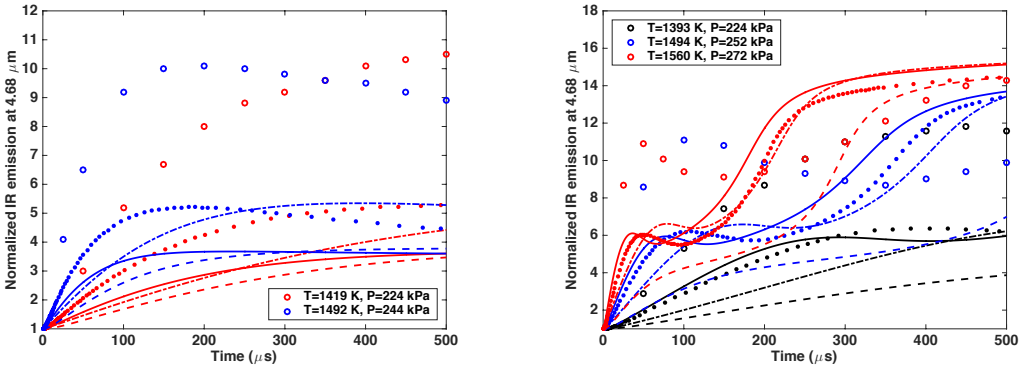

a) Emission at 4.68 μm for mixture 19 b) Emission at 4.68 μm for mixture 17

Figure 10: Comparison between the experimental [6] and the predicted emission at 4.68 μm profiles during the pyrolysis (a) and oxidation (b) of CH_3CHO. Solid lines: present model; Dashed-dotted lines: Aramco 2.0; Dotted lines: CaltechMech; Dashed lines: JetSurf.

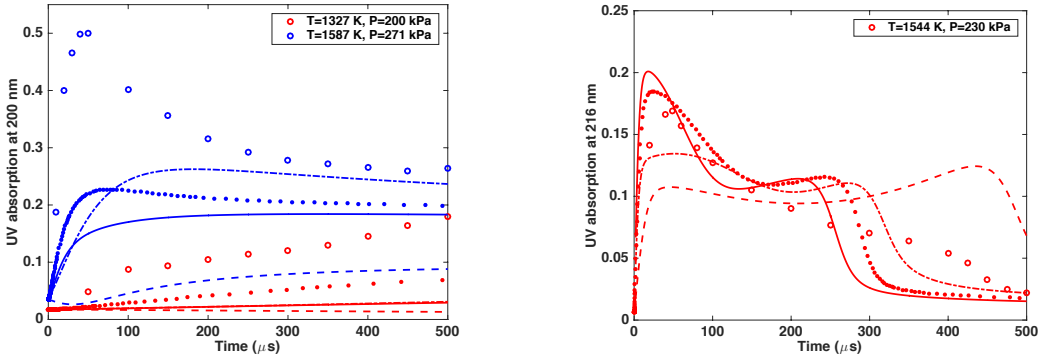

a) Absorption at 200 nm for mixture 19 b) Absorption at 216 nm for mixture 14

Figure 11: Comparison between the experimental [6] and the predicted absorption at 200-216 nm profiles during the pyrolysis (a) and oxidation (b) of CH_3CHO. Solid lines: present model; Dashed-dotted lines: Aramco 2.0; Dotted lines: CaltechMech; Dashed lines: JetSurf.

References

[1] Y. Li, C.-W. Zhou, K. Somers, K. Zhang, H. Curran, Proceedings of the Combustion Institute 36 (2017) 403–411.

[2] G. Blanquart, P. Pepiot-Desjardins, H. Pitsch, Combustion and Flame 156 (2009) 588–607.

[3] B. Sirjean, E. Dames, D. A. Sheen, X.-Q. You, C. Sung, A. T. Holley, F. N. Egolfopoulos, H. Wang, S. S. Vasu, D. F. Davidson, R. K. Hanson, H. Pitsch, C. T. Bowman, A. Kelley, C. K. Law, W. Tsang, N. P. Cernansky, D. L. Miller, A. Violi, R. P. Lindstedt, A high-temperature chemical kinetic model of n-alkane oxidation, jetsurf version 0.2,, Available at: $http://melchior.usc.edu/JetSurF/Version0_2/Index.html$, 2008.

[4] P. Dagaut, M. Reuillon, D. Voisin, M. Cathonnet, M. M. Guinness, J. Simmie, Combustion Science and Technology 107 (1995) 301–316.

[5] Y. Hidaka, M. Suga, Journal of the Mass Spectrometry Society of Japan 35 (1987) 74–83.

[6] K. Yasunaga, S. Kubo, H. Hoshikawa, T. Kamesawa, Y. Hidaka, International Journal of Chemical Kinetics 40 (2008) 73–102.

[7] S. Wang, D. Davidson, R. Hanson, Combustion and Flame 160 (2013) 1930–1938.

[8] S. Wang, D. Davidson, R. Hanson, Journal of Physical Chemistry A In press (2016).

[9] R. Sivaramakrishnan, J. V. Michael, S. J. Klippenstein, The Journal of Physical Chemistry A 114 (2010) 755–764.

[10] T. Bentz, F. Striebel, , M. Olzmann, Journal of Physical Chemistry A 112 (2008) 6120–6124.

[11] R. Kern, H. Singh, K. Xie, AIP Conference Proceedings 208 (1990) 487–492.